

UC Davis

UC Davis Previously Published Works

Title

Reduced difference polynomials and self-intersection computations

Permalink

<https://escholarship.org/uc/item/87p3w1dg>

Journal

Applied Mathematics and Computation, 324(C)

ISSN

0096-3003

Author

Farouki, Rida T

Publication Date

2018-05-01

DOI

10.1016/j.amc.2017.12.016

Peer reviewed

Reduced difference polynomials and self–intersection computations

Rida T. Farouki

Department of Mechanical and Aerospace Engineering,
University of California, Davis, CA 95616, USA.

Abstract

A *reduced difference polynomial* $f(u, v) = (p(u) - p(v)) / (u - v)$ may be associated with any given univariate polynomial $p(t)$, $t \in [0, 1]$ such that the locus $f(u, v) = 0$ identifies the pairs of *distinct* values u and v satisfying $p(u) = p(v)$. The Bernstein coefficients of $f(u, v)$ on $[0, 1]^2$ can be determined from those of $p(t)$ through a simple algorithm, and can be restricted to any subdomain of $[0, 1]^2$ by standard subdivision methods. By constructing the reduced difference polynomials $f(u, v)$ and $g(u, v)$ associated with the coordinate components of a polynomial curve $\mathbf{r}(t) = (x(t), y(t))$, a quadtree decomposition of $[0, 1]^2$ guided by the variation–diminishing property yields a numerically stable scheme for isolating real solutions of the system $f(u, v) = g(u, v) = 0$, which identify self–intersections of the curve $\mathbf{r}(t)$. Through the Kantorovich theorem for guaranteed convergence of Newton–Raphson iterations to a unique solution, the self–intersections can be efficiently computed to machine precision. By generalizing the reduced difference polynomial to encompass products of univariate polynomials, the method can be readily extended to compute the self–intersections of rational curves, and of the rational offsets to Pythagorean–hodograph curves.

Keywords: Bernstein basis; polynomial division; variation–diminishing property; quadtree decomposition; Kantorovich theorem; polynomial curves; rational curves; self–intersections; Pythagorean–hodograph curves; offset curve trimming.

e–mail address: farouki@ucdavis.edu

1 Introduction

The Bernstein form of a polynomial over a finite domain has found widespread application in diverse contexts, on account of its numerical stability and the intuitive and versatile algorithms it entails [5]. Methods for generalizing the Bernstein form, and for deriving new properties and algorithms, continue to be active areas of investigation [14, 21]. In the present study, we investigate the use of the Bernstein form in developing robust algorithms to address the problem of computing the self-intersections of planar curves.

With any univariate polynomial $p(t)$, we may associate a bivariate *reduced difference polynomial* $f(u, v) = (p(u) - p(v))/(u - v)$, such that the points of the algebraic curve $f(u, v) = 0$ identify the pairs of *distinct* values u and v of the independent variable t that satisfy $p(u) = p(v)$. When $p(t)$ is specified in Bernstein form on $t \in [0, 1]$, the Bernstein coefficients of the tensor-product form of $f(u, v)$ on $(u, v) \in [0, 1] \times [0, 1]$ can be easily obtained from those of $p(t)$, and can be specialized to any rectangular subdomain $[u_1, u_2] \times [v_1, v_2]$ by standard subdivision algorithms. These ideas also generalize to a product $p_1(t) p_2(t)$ of polynomials, in which case the reduced difference polynomial is defined as $f(u, v) = (p_1(u) p_2(v) - p_1(v) p_2(u))/(u - v)$.

The construction of reduced difference polynomials, in conjunction with the subdivision and variation-diminishing properties of the Bernstein form, offers an efficient and extremely robust means of isolating and computing the self-intersections of planar polynomial and rational curves, and also of the offsets to planar Pythagorean-hodograph (PH) curves, which are essential to the offset trimming process. All these problems can be reduced to computing the intersections on $(u, v) \in [0, 1] \times [0, 1]$ of two algebraic curves $f(u, v) = 0$ and $g(u, v) = 0$, specified by two reduced difference polynomials.

The intersection points of $f(u, v) = 0$ and $g(u, v) = 0$ can be isolated by use of a quadtree decomposition of the domain $[0, 1] \times [0, 1]$ guided by both of these curves. Invoking the variation-diminishing property of the Bernstein form, any subdomain $[u_1, u_2] \times [v_1, v_2]$ on which the coefficients of $f(u, v)$ or $g(u, v)$ are all of the same sign can be discarded as not containing a portion of both curves. Since the quadtree decomposition is governed by *both* curves, it rapidly converges on a set of small subdomains that (potentially) enclose intersection points of $f(u, v) = 0$ and $g(u, v) = 0$, and an efficient test for the guaranteed convergence of Newton-Raphson iterations to a unique solution within such subdomains allows their rapid computation to machine precision, once they are sufficiently isolated. Since the quadtree subdivision procedure

incurs taking only convex combinations of the original Bernstein coefficients of $f(u, v)$ and $g(u, v)$, the method is numerically stable and robust.

Instead of attempting a “synthetic division” of $p(u) - p(v)$ by $u - v$, we formulate a simple recursive algorithm to determine the Bernstein coefficients of $f(u, v)$ from those of $p(t)$. Organizing these coefficients into a matrix, the “boundary” elements are first populated through simple expressions, and the “interior” elements can then be recursively filled in, row-by-row. The process can be further simplified by noting that, since $f(u, v) = f(v, u)$, this matrix is symmetric. It should be noted that the self-intersection algorithms described herein can also be readily adapted to computing the mutual intersections of distinct curves, by considering the bivariate form $p_1(u) - p_2(v)$ for *different* polynomials $p_1(t)$ and $p_2(t)$, and omitting the division by $u - v$.

The remainder of this paper is organized as follows. Section 2 describes the construction of the bivariate difference polynomial associated with a given univariate polynomial. Section 3 then shows how its Bernstein coefficients on any given subdomain $[u_1, u_2] \times [v_1, v_2] \subset [0, 1] \times [0, 1]$ can be obtained by matrix multiplications. These results are used in Section 4 to generate a quadtree decomposition of $(u, v) \in [0, 1] \times [0, 1]$ to a prescribed resolution, governed by reduced difference polynomials $f(u, v) = 0$ and $g(u, v) = 0$ that characterize the self-intersections of planar polynomial curves. A generalized form of the reduced difference polynomial is introduced in Sections 5 and 6, and applied to computing the self-intersections of rational curves, and of the offsets to Pythagorean-hodograph curves. Finally, Section 7 summarizes the methodology proposed herein and suggests possible further developments. The Kantorovich theorem guaranteeing convergence of the Newton-Raphson iteration to a unique solution of the system $f(u, v) = g(u, v) = 0$, within a given subdomain, is briefly discussed in an Appendix.

2 Reduced difference polynomials

For any specified univariate polynomial $p(t)$, a bivariate *difference polynomial* $q(u, v) := p(u) - p(v)$ may be defined, whose value is the difference between $p(t)$ at $t = u$ and $t = v$. Since $q(u, v)$ obviously vanishes when $u = v$, it must contain the factor $u - v$. Therefore, $f(u, v) := q(u, v)/(u - v)$ is a polynomial of lower degree, that does not vanish when $u = v$, and the locus $f(u, v) = 0$ identifies pairs of *distinct* (u, v) values such that $p(u) = p(v)$. We call $f(u, v)$ the *reduced* difference polynomial associated with $p(t)$.

In dealing with polynomials on finite domains, it is desirable to employ the Bernstein representation, on account of its numerical stability and the many advantageous properties and useful algorithms it entails [5]. The Bernstein basis of degree n on the domain $t \in [0, 1]$ is defined by

$$b_i^n(t) := \binom{n}{i} (1-t)^{n-i} t^i, \quad i = 0, \dots, n, \quad (1)$$

and a degree- n polynomial $p(t)$ is specified by Bernstein coefficients a_0, \dots, a_n as

$$p(t) = \sum_{i=0}^n a_i b_i^n(t).$$

The basis (1) satisfies the partition-of-unity property

$$\sum_{i=0}^n b_i^n(t) \equiv 1, \quad (2)$$

which can be used to write $q(u, v) := p(u) - p(v)$ in the tensor-product form

$$q(u, v) = \sum_{j=0}^n a_j b_j^n(u) - \sum_{k=0}^n a_k b_k^n(v) = \sum_{j=0}^n \sum_{k=0}^n (a_j - a_k) b_j^n(u) b_k^n(v). \quad (3)$$

Since $q(u, v)$ contains the factor $u - v$, dividing it out yields a polynomial of the form

$$f(u, v) := \frac{q(u, v)}{u - v} = \sum_{j=0}^{n-1} \sum_{k=0}^{n-1} c_{jk} b_j^{n-1}(u) b_k^{n-1}(v). \quad (4)$$

To determine the coefficients c_{jk} of $f(u, v)$ for $0 \leq j, k \leq n - 1$, we express the linear factor $u - v$ in Bernstein form as

$$u - v = b_1^1(u) b_0^1(v) - b_0^1(u) b_1^1(v).$$

Then from (3) and (4) we must have

$$\begin{aligned} \sum_{j=0}^n \sum_{k=0}^n (a_j - a_k) b_j^n(u) b_k^n(v) = \\ [b_1^1(u) b_0^1(v) - b_0^1(u) b_1^1(v)] \sum_{j=0}^{n-1} \sum_{k=0}^{n-1} c_{jk} b_j^{n-1}(u) b_k^{n-1}(v). \end{aligned} \quad (5)$$

To facilitate a term-by-term comparison of the left and right hand sides, we note that

$$b_1^1(u) b_0^1(v) b_j^{n-1}(u) b_k^{n-1}(v) = \frac{(j+1)(n-k)}{n^2} b_{j+1}^n(u) b_k^n(v),$$

$$b_0^1(u) b_1^1(v) b_j^{n-1}(u) b_k^{n-1}(v) = \frac{(n-j)(k+1)}{n^2} b_j^n(u) b_{k+1}^n(v).$$

Substituting these relations, the expression on the right in (5) becomes

$$\sum_{j=0}^{n-1} \sum_{k=0}^{n-1} \frac{(j+1)(n-k)}{n^2} c_{jk} b_{j+1}^n(u) b_k^n(v) - \frac{(n-j)(k+1)}{n^2} c_{jk} b_j^n(u) b_{k+1}^n(v),$$

and by a change of summation indices, this can be re-formulated as

$$\sum_{j=1}^n \sum_{k=0}^{n-1} \frac{j(n-k)}{n^2} c_{j-1,k} b_j^n(u) b_k^n(v) - \sum_{j=0}^{n-1} \sum_{k=1}^n \frac{(n-j)k}{n^2} c_{j,k-1} b_j^n(u) b_k^n(v).$$

Now each term of (3) with j or k equal to 0 or n has only one corresponding term in the above expression, while all terms with $1 \leq j, k \leq n-1$ have two corresponding terms. Equating these corresponding terms, the “boundary” coefficients of (4) are given by

$$\begin{aligned} c_{0,k} &= \frac{n}{k+1} (a_{k+1} - a_0), \quad k = 0, \dots, n-1, \\ c_{n-1,k} &= \frac{n}{n-k} (a_n - a_k), \quad k = 0, \dots, n-1, \\ c_{j,0} &= \frac{n}{j+1} (a_{j+1} - a_0), \quad j = 0, \dots, n-1, \\ c_{j,n-1} &= \frac{n}{n-j} (a_n - a_j), \quad j = 0, \dots, n-1, \end{aligned}$$

and once they have been assigned, the “interior” coefficients may be obtained for rows $j = 1, \dots, n-2$ using

$$c_{j,k-1} = \frac{j(n-k)}{(n-j)k} c_{j-1,k} - \frac{n^2}{(n-j)k} (a_j - a_k), \quad 2 \leq k \leq n-1.$$

Note that the resulting coefficient matrix $\{c_{jk}\}$, $0 \leq j, k \leq n-1$ is symmetric, reflecting the symmetry property $f(u, v) = f(v, u)$ of the polynomial (4).

3 Subdivision scheme

The equation $f(u, v) = 0$ determines an implicit curve in the domain $(u, v) \in [0, 1] \times [0, 1]$. A *quadtrees* decomposition of this domain, in conjunction with the *variation–diminishing property* of the Bernstein form, offers a stable and efficient means of characterizing the topological configuration of this curve. The quadtree decomposition is discussed in Section 4 below. The variation–diminishing property states that a subdomain $[u_1, u_2] \times [v_1, v_2]$ contains no part of the curve $f(u, v) = 0$ if the Bernstein coefficients of (4) appropriate to that subdomain are all of the same sign.

The degree– n Bernstein basis on a general interval $[t_1, t_2]$ is defined by

$$\bar{b}_i^n(t) = \binom{n}{i} \frac{(t_2 - t)^{n-i} (t - t_1)^i}{(t_2 - t_1)^n}, \quad i = 0, \dots, n. \quad (6)$$

The basis (1) on $[0, 1]$ is related [8] to the basis (6) by an $(n + 1) \times (n + 1)$ matrix \mathbf{M} with elements

$$M_{jk} = \sum_{i=\max(0, j+k-n)}^{\min(j, k)} b_{k-i}^{n-j}(t_1) b_i^j(t_2), \quad 0 \leq j, k \leq n \quad (7)$$

through the expression

$$b_k^n(t) = \sum_{j=0}^n \bar{b}_j^n(t) M_{jk}, \quad k = 0, \dots, n.$$

Consequently, the coefficients for the Bernstein representations

$$p(t) = \sum_{i=0}^n a_i b_i^n(t) = \sum_{i=0}^n \bar{a}_i \bar{b}_i^n(t)$$

on $[0, 1]$ and $[t_1, t_2]$ are related by

$$\bar{a}_i = \sum_{r=0}^n M_{ir} a_r, \quad i = 0, \dots, n.$$

When $[t_1, t_2] \subset [0, 1]$ the elements (7) define a *stochastic matrix* [10] — i.e., they are all non–negative, and sum to unity across each row. Consequently,

the coefficients \bar{a}_i are all *convex combinations* of the coefficients a_i , and their computation is inherently very stable.

To obtain the coefficients \bar{c}_{jk} of the bivariate tensor-product polynomial (4) on a subdomain $[u_1, u_2] \times [v_1, v_2]$ from the coefficients c_{jk} on $[0, 1] \times [0, 1]$ we construct $n \times n$ subdivision matrices appropriate to bases of degree $n - 1$ and intervals $[u_1, u_2]$ and $[v_1, v_2]$. These matrices are defined by the elements

$$U_{jk} = \sum_{i=\max(0, j+k-n+1)}^{\min(j, k)} b_{k-i}^{n-1-j}(u_1) b_i^j(u_2)$$

$$V_{jk} = \sum_{i=\max(0, j+k-n+1)}^{\min(j, k)} b_{k-i}^{n-1-j}(v_1) b_i^j(v_2),$$

for $0 \leq j, k \leq n - 1$. In terms of them, the Bernstein coefficients of (4) on the subdomain $[u_1, u_2] \times [v_1, v_2]$ are obtained as

$$\bar{c}_{jk} = \sum_{r=0}^{n-1} \sum_{s=0}^{n-1} U_{jr} V_{ks} c_{rs}, \quad 0 \leq j, k \leq n - 1. \quad (8)$$

4 Self-intersection of polynomial curves

Quadtree decomposition [17, 18] can be employed to generate a hierarchical characterization of an implicit curve $f(u, v) = 0$ within the domain $(u, v) \in [0, 1] \times [0, 1]$. The domain is first subdivided into four quadrants, along the lines $u = \frac{1}{2}$ and $v = \frac{1}{2}$, and the signs of the coefficients (8) appropriate to each quadrant are checked for (potential) occupancy by the curve $f(u, v) = 0$. Those that fail this test are flagged “empty” and are discarded from further consideration, while those that pass are subdivided into subquadrants, each of which is again subject to the occupancy test. This hierarchical subdivision process is repeated to some desired level r of resolution, the outcome being a set of (potentially) occupied subdomains of side length 2^{-r} that localize the curve $f(u, v) = 0$ within the overall domain $[0, 1] \times [0, 1]$.

This provides an efficient and robust method for isolating self-intersections a plane polynomial curve $\mathbf{r}(t) = (x(t), y(t))$, $t \in [0, 1]$. Let

$$f(u, v) = \frac{x(u) - x(v)}{u - v} \quad \text{and} \quad g(u, v) = \frac{y(u) - y(v)}{u - v} \quad (9)$$

be reduced difference polynomials for $x(t)$ and $y(t)$, constructed as described in Section 2. Then the intersections of the loci $f(u, v) = 0$ and $g(u, v) = 0$ within $[0, 1] \times [0, 1]$ identify the parameter values of the self-intersections of the curve $\mathbf{r}(t)$, such that $\mathbf{r}(u) = \mathbf{r}(v)$. In the domain decomposition process, only subdomains over which *both* the polynomials (9) exhibit sign changes in their coefficients are retained. Moreover, since these polynomials exhibit the symmetry property $f(u, v) = f(v, u)$ and $g(u, v) = g(v, u)$, each solution (u, v) of $f(u, v) = g(u, v) = 0$ has a counterpart (v, u) that identifies the same self-intersection point of $\mathbf{r}(t)$. Hence, to avoid duplication, we can eliminate from consideration all subdomains that lie either entirely below or entirely above the line $u = v$. The Kantorovich theorem (see the Appendix) allows solutions that are isolated in sufficiently small subdomains to be efficiently computed to machine precision by Newton–Raphson iterations.

Example 1 A simple example suffices to illustrate the basic methodology. Consider the cubic $\mathbf{r}(t) = (x(t), y(t))$ defined by the Bézier control points

$$\begin{aligned} \mathbf{p}_0 &= (2.000000, 1.000000), & \mathbf{p}_1 &= (3.200000, 3.078461), \\ \mathbf{p}_2 &= (0.523148, 2.361201), & \mathbf{p}_3 &= (3.294429, 0.761201). \end{aligned}$$

This curve has a single self-intersection — see Figure 2 below. In this case, the reduced difference polynomials $f(u, v)$ and $g(u, v)$ obtained from $x(t)$ and $y(t)$ are biquadratic, specified by the Bernstein coefficients

$$\begin{aligned} & \begin{bmatrix} 3.600000 & -2.215278 & 1.294429 \\ -2.215278 & -5.699310 & 0.141644 \\ 1.294429 & 0.141644 & 8.313844 \end{bmatrix}, \\ & \begin{bmatrix} 6.235383 & 2.041801 & -0.238799 \\ 2.041801 & -1.673536 & -3.475891 \\ -0.238799 & -3.475891 & -4.800000 \end{bmatrix}. \end{aligned}$$

Figure 1 illustrates the quadtree localizations¹ (to a resolution of 2^{-7}) of the two curves $f(u, v) = 0$ and $g(u, v) = 0$, which are evidently symmetric about the diagonal line $u = v$. The simultaneous combination of these two quadtree decompositions leads to a very rapid isolation of the solutions to the system $f(u, v) = g(u, v) = 0$ in the unit square, as seen in Figure 2.

¹In all the examples, we show the individual quadtree localizations of $f(u, v) = 0$ and $g(u, v) = 0$ only as visualization aids: the algorithm does not use them individually.

For the chosen 2^{-7} quadtree resolution, the only subdomains over which $f(u, v)$ and $g(u, v)$ both exhibit sign changes in their coefficients are

$$\left[\frac{12}{128}, \frac{14}{128} \right] \times \left[\frac{104}{128}, \frac{105}{128} \right] \quad \text{and} \quad \left[\frac{104}{128}, \frac{105}{128} \right] \times \left[\frac{12}{128}, \frac{14}{128} \right]$$

above and below the line $u = v$, respectively. Choosing the midpoint $(u, v) = (13/128, 209/256)$ of the former as a starting approximation, a few Newton–Raphson iterations yield convergence to machine precision for the parameter values identifying the self–intersection, namely $(u, v) = (0.101425, 0.814535)$.

Example 2 As a more challenging example, we consider the quintic $\mathbf{r}(t) = (x(t), y(t))$ specified by the Bézier control points

$$\begin{aligned} \mathbf{p}_0 &= (2.9, 0.8), & \mathbf{p}_1 &= (3.3, 3.8), & \mathbf{p}_2 &= (1.0, 1.0), \\ \mathbf{p}_3 &= (4.5, 1.0), & \mathbf{p}_4 &= (2.9, 3.2), & \mathbf{p}_5 &= (1.9, 1.0). \end{aligned}$$

As seen in Figure 4 below, this curve has three self–intersections. The reduced difference polynomials $f(u, v)$ and $g(u, v)$ obtained from $x(t)$ and $y(t)$ in this case are biquartic, with the coefficients

$$\begin{aligned} & \begin{bmatrix} 2.000000 & -4.750000 & 2.666667 & 0.000000 & -1.000000 \\ -4.750000 & -6.187500 & 2.500000 & -0.687500 & -1.750000 \\ 2.666667 & 2.500000 & 9.416667 & 3.666667 & 1.500000 \\ 0.000000 & -0.687500 & 3.666667 & -4.437500 & -6.500000 \\ -1.000000 & -1.750000 & 1.500000 & -6.500000 & -5.000000 \end{bmatrix}, \\ & \begin{bmatrix} 15.000000 & 0.500000 & 0.333333 & 3.000000 & 0.200000 \\ 0.500000 & -8.625000 & -5.333333 & -0.925000 & -3.500000 \\ 0.333333 & -5.333333 & -0.411111 & 4.000000 & 0.000000 \\ 3.000000 & -0.925000 & 4.000000 & 6.875000 & 0.000000 \\ 0.200000 & -3.500000 & 0.000000 & 0.000000 & -11.000000 \end{bmatrix}. \end{aligned}$$

Figure 3 shows the quadtree localizations of $f(u, v) = 0$ and $g(u, v) = 0$, with resolution 2^{-7} . Using both to govern the subdivision, the only subdomains over which $f(u, v)$ and $g(u, v)$ both exhibit coefficient sign changes are

$$\left[\frac{12}{128}, \frac{13}{128} \right] \times \left[\frac{69}{128}, \frac{71}{128} \right], \quad \left[\frac{15}{128}, \frac{16}{128} \right] \times \left[\frac{98}{128}, \frac{100}{128} \right], \quad \left[\frac{49}{128}, \frac{51}{128} \right] \times \left[\frac{106}{128}, \frac{107}{128} \right]$$

above the line $u = v$, with symmetric subdomains below this line. Taking the midpoints of these subdomains as starting approximations, Newton–Raphson iterations again converge rapidly to machine precision, yielding the pairs of parameter values $(u, v) = (0.093976, 0.551966)$, $(u, v) = (0.123767, 0.774180)$, and $(u, v) = (0.390536, 0.833024)$ identifying the three self–intersection points, which are illustrated in Figure 4.

5 Self–intersections of rational curves

As observed in Section 1, the concept of a reduced difference polynomial may be generalized to accommodate the *products* of polynomials. We show here how this generalization is useful in developing self–intersection algorithms for rational curves, and for the offsets to PH curves in Section 6.

Rational forms are universally employed in computer–aided design, since they admit *exact* representations of conic curves, quadric surfaces, surfaces of revolution, and other basic geometrical forms, and they also exhibit closure under projective transformations [3]. For a degree– n rational curve

$$\mathbf{r}(t) = \left(\frac{X(t)}{W(t)}, \frac{Y(t)}{W(t)} \right)$$

specified by homogeneous coordinate polynomials $W(t), X(t), Y(t)$ we may form the bivariate reduced difference polynomials

$$f(u, v) = \frac{W(v)X(u) - W(u)X(v)}{u - v}, \quad g(u, v) = \frac{W(v)Y(u) - W(u)Y(v)}{u - v}.$$

If the Bézier control points of $\mathbf{r}(t)$ have homogeneous coordinates (w_i, x_i, y_i) for $i = 0, \dots, n$ we obtain

$$W(v)X(u) - W(u)X(v) = \sum_{j=0}^n \sum_{k=0}^n (w_k x_j - w_j x_k) b_j^n(u) b_k^n(v),$$

with an analogous expression for $W(v)Y(u) - W(u)Y(v)$. Thus, writing

$$f(u, v) = \sum_{j=0}^{n-1} \sum_{k=0}^{n-1} c_{jk} b_j^{n-1}(u) b_k^{n-1}(v),$$

we must have

$$\sum_{j=0}^n \sum_{k=0}^n (w_k x_j - w_j x_k) b_j^n(u) b_k^n(v) = [b_1^1(u) b_0^1(v) - b_0^1(u) b_1^1(v)] \sum_{j=0}^{n-1} \sum_{k=0}^{n-1} c_{jk} b_j^{n-1}(u) b_k^{n-1}(v).$$

Thus, by arguments analogous to those of Section 2, we obtain the boundary coefficients

$$\begin{aligned} c_{0,k} &= \frac{n}{k+1} (w_0 x_{k+1} - w_{k+1} x_0), \quad k = 0, \dots, n-1, \\ c_{n-1,k} &= \frac{n}{n-k} (w_k x_n - w_n x_k), \quad k = 0, \dots, n-1, \\ c_{j,0} &= \frac{n}{j+1} (w_0 x_{j+1} - w_{j+1} x_0), \quad j = 0, \dots, n-1, \\ c_{j,n-1} &= \frac{n}{n-j} (w_j x_n - w_n x_j), \quad j = 0, \dots, n-1, \end{aligned}$$

and the “interior” coefficients are obtained for rows $j = 1, \dots, n-2$ using

$$c_{j,k-1} = \frac{j(n-k)}{(n-j)k} c_{j-1,k} - \frac{n^2}{(n-j)k} (w_k x_j - w_j x_k), \quad 2 \leq k \leq n-1.$$

The coefficients of the reduced difference polynomial $g(u, v)$ can be obtained by simply substituting y_0, \dots, y_n for x_0, \dots, x_n in the preceding expressions for the coefficients of $f(u, v)$.

Example 3 Consider a rational quintic curve specified by the same control points $\mathbf{p}_0, \dots, \mathbf{p}_5$ as in Example 2, but with the associated weights

$$w_0 = 0.4, \quad w_1 = 1.2, \quad w_2 = 1.8, \quad w_3 = 2.4, \quad w_4 = 1.2, \quad w_5 = 0.4.$$

This curve has three self-intersections (see Figure 6 below), and the reduced difference polynomials $f(u, v)$ and $g(u, v)$ are biquartic, with the coefficients

$$\begin{bmatrix} 0.960000 & -3.420000 & 2.560000 & 0.000000 & -0.160000 \\ -3.420000 & -14.565000 & 7.200000 & -0.910000 & -0.840000 \\ 2.560000 & 7.200000 & 41.595556 & 8.410000 & 1.080000 \\ 0.000000 & -0.910000 & 8.410000 & -13.995000 & -6.240000 \\ -0.160000 & -0.840000 & 1.080000 & -6.240000 & -2.400000 \end{bmatrix},$$

$$\begin{bmatrix} 7.200000 & 0.360000 & 0.320000 & 1.440000 & 0.032000 \\ 0.360000 & -18.780000 & -16.560000 & -1.348000 & -1.680000 \\ 0.320000 & -16.560000 & -0.599111 & 9.620000 & 0.000000 \\ 1.440000 & -1.348000 & 9.620000 & 19.800000 & 0.000000 \\ 0.032000 & -1.680000 & 0.000000 & 0.000000 & 5.280000 \end{bmatrix}.$$

Figure 5 shows the quadtree localizations of $f(u, v) = 0$ and $g(u, v) = 0$, with resolution 2^{-7} . Using both to govern the subdivision, the only subdomains over which $f(u, v)$ and $g(u, v)$ both exhibit coefficient sign changes are

$$\left[\frac{0}{128}, \frac{1}{128} \right] \times \left[\frac{14}{128}, \frac{16}{128} \right], \left[\frac{1}{128}, \frac{2}{128} \right] \times \left[\frac{28}{128}, \frac{29}{128} \right], \left[\frac{8}{128}, \frac{10}{128} \right] \times \left[\frac{30}{128}, \frac{31}{128} \right]$$

above the line $u = v$, with symmetric subdomains below this line. Taking the midpoints of these subdomains as starting approximations, a few Newton–Raphson iterations again converge to machine precision, yielding the pairs of parameter values $(u, v) = (0.093976, 0.551966)$, $(u, v) = (0.123767, 0.774180)$, and $(u, v) = (0.390536, 0.833024)$ identifying the three self–intersection points, which are illustrated in Figure 6.

The following example shows that the algorithm can also accommodate self–intersections of higher order. It is well known that an “ordinary” m –fold point (i.e., a point that the curve traverses m times, with *distinct* tangents) is equivalent to $\frac{1}{2}m(m-1)$ double points. In the presence of an m –fold point, the algorithm will identify $\frac{1}{2}m(m-1)$ pairs of parameter values, all of which generate the same Cartesian point upon evaluation of the curve.

Example 4 Consider the rational quartic curve defined by the weights and control points

$$\begin{aligned} w_0 &= 169, & \mathbf{p}_0 &= (-108, -18\sqrt{3})/169, \\ w_1 &= -143, & \mathbf{p}_1 &= (-144, -15\sqrt{3})/143, \\ w_2 &= 137, & \mathbf{p}_2 &= (-156, 0)/137, \\ w_3 &= -143, & \mathbf{p}_3 &= (-144, 15\sqrt{3})/143, \\ w_4 &= 169, & \mathbf{p}_4 &= (-108, 18\sqrt{3})/169. \end{aligned}$$

This curve has a triple point at the origin, corresponding to the three distinct parameter values $t = \frac{1}{4}, \frac{1}{2}, \frac{3}{4}$ (Figure 8). The reduced difference polynomials

$f(u, v)$ and $g(u, v)$ in this case are bicubic, with the coefficients

$$\begin{bmatrix} 35568.00 & -23136.00 & 11856.00 & 0.00 \\ -23136.00 & 10832.00 & 0.00 & -11856.00 \\ 11856.00 & 0.00 & -10832.00 & 23136.00 \\ 0.00 & -11856.00 & 23136.00 & -35568.00 \end{bmatrix},$$

$$\begin{bmatrix} -270.20 & 8542.47 & -11798.73 & 10537.80 \\ 8542.47 & -13424.55 & 14380.64 & -11798.73 \\ -11798.73 & 14380.64 & -13424.55 & 8542.47 \\ 10537.80 & -11798.73 & 8542.47 & -270.20 \end{bmatrix}.$$

Figure 7 shows the quadtree localizations of $f(u, v) = 0$ and $g(u, v) = 0$, with resolution 2^{-7} . Using both to govern the subdivision, the only subdomains over which $f(u, v)$ and $g(u, v)$ both exhibit coefficient sign changes cluster around the pairs $(\frac{1}{4}, \frac{1}{2})$, $(\frac{1}{2}, \frac{3}{4})$, $(\frac{1}{4}, \frac{3}{4})$ above the line $u = v$, which identify the triple point regarded as the coalescence of three double points (see Figure 8). A few Newton–Raphson iterations yield convergence to machine precision, and evaluating the curve gives $\mathbf{r}(\frac{1}{4}) = \mathbf{r}(\frac{1}{2}) = \mathbf{r}(\frac{3}{4})$, indicating that this point is, in fact, a triple point rather than three distinct double points.

The computation of non–ordinary self–intersections (multiple traversals of a single point with two or more coincident tangents) is a singular problem, that is numerically ill–conditioned. A robust treatment of such problems will require special methods, which we shall not attempt to address at present.

6 Self–intersections of PH curve offsets

The distinctive feature of a planar polynomial Pythagorean–hodograph (PH) curve $\mathbf{r}(t) = (x(t), y(t))$ is that its derivative $\mathbf{r}'(t) = (x'(t), y'(t))$ satisfies, for some polynomial $\sigma(t)$, the condition

$$x'^2(t) + y'^2(t) \equiv \sigma^2(t).$$

The polynomial $\sigma(t) = |\mathbf{r}'(t)|$ specifies the derivative of the arc length s with respect to the parameter t , and is called the *parametric speed* of the PH curve. Consequently, $\mathbf{r}(t)$ has a *rational* unit normal $\mathbf{n}(t) = (y'(t), -x'(t))/\sigma(t)$ and the *offset curves*

$$\mathbf{r}_d(t) = \mathbf{r}(t) + d\mathbf{n}(t) \tag{10}$$

at each (signed) distance d from $\mathbf{r}(t)$ are *rational curves* [9].

The locus (10) defines the *untrimmed offset* to $\mathbf{r}(t)$ — each point of $\mathbf{r}_d(t)$ is distance d from the corresponding point of $\mathbf{r}(t)$, but not necessarily distance d from *every* point of $\mathbf{r}(t)$. The locus with the latter property is known as the *trimmed offset*, and it can be obtained [6] by deleting certain segments of $\mathbf{r}_d(t)$ delineated by parameter values corresponding to self-intersections.

The computation of the self-intersections of $\mathbf{r}_d(t)$ is a difficult problem. Algebraic methods, based on elimination theory, are rather cumbersome and incur high degree polynomials [1, 7] whose roots may be difficult to accurately compute in finite-precision arithmetic. Level set methods [2, 16, 20] bypass the need for trimming, by treating the offset curve as the numerical solution of a partial differential equation, but are limited in accuracy by the adopted grid resolution. Pre-computation of the Voronoi diagram for a given domain boundary obviates the need for offset trimming [11, 12] since the trimmed offset segments begin and end on the Voronoi diagram edges. However, exact computations of Voronoi diagrams are limited to simple (linear or circular) boundary segments. Other methods, based [13, 19] on distance fields, employ *a priori* approximations of the given curve $\mathbf{r}(t)$ or its untrimmed offset $\mathbf{r}_d(t)$. The approach described below, based upon reduced difference polynomials, circumvents many limitations of these existing methods by combining the robust and efficient properties of the Bernstein representation and quadtree decomposition, using only the exact definition of the given curve $\mathbf{r}(t)$.

The untrimmed offset (10) to a degree- n PH curve is a rational curve of degree $2n - 1$. Explicit expressions for its control points and weights were formulated in [9] for the cases $n = 3$ and $n = 5$. Based on these expressions, the approach described in Section 5 can, in principle, be directly applied to compute the offset self-intersections. A different approach is employed here, avoiding the need to explicitly compute the offset control points and weights, and instead using only the low-degree polynomials $x'(t), y'(t), \sigma(t)$.

Self-intersections of the offset curve (10) are identified by pairs of distinct values u, v of the parameter t , such that

$$\mathbf{r}(u) + d\mathbf{n}(u) = \mathbf{r}(v) + d\mathbf{n}(v) \quad (11)$$

For a regular PH curve $\mathbf{r}(t) = (x(t), y(t))$ of degree n , with parametric speed satisfying $\sigma(t) \neq 0$ for $t \in [0, 1]$, these pairs correspond to solutions of the

polynomial equations

$$\begin{aligned} f(u, v) &:= \sigma(u)\sigma(v)\frac{x(u) - x(v)}{u - v} + d\frac{\sigma(v)y'(u) - \sigma(u)y'(v)}{u - v} = 0, \\ g(u, v) &:= \sigma(u)\sigma(v)\frac{y(u) - y(v)}{u - v} - d\frac{\sigma(v)x'(u) - \sigma(u)x'(v)}{u - v} = 0. \end{aligned} \quad (12)$$

We consider only the construction of $f(u, v)$, since the construction of $g(u, v)$ is closely analogous. In the first term of $f(u, v)$ we may write

$$\frac{x(u) - x(v)}{u - v} = \sum_{j=0}^{n-1} \sum_{k=0}^{n-1} \alpha_{jk} b_j^{n-1}(u) b_k^{n-1}(v),$$

the coefficients α_{jk} being determined as described in Section 2. Then, using the product rule [5] for polynomials in Bernstein form, the first term may be expressed as

$$\sigma(u)\sigma(v)\frac{x(u) - x(v)}{u - v} = \sum_{j=0}^{2n-2} \sum_{k=0}^{2n-2} \beta_{jk} b_j^{2n-2}(u) b_k^{2n-2}(v)$$

with coefficients defined for $0 \leq j, k \leq 2n - 2$ by

$$\beta_{jk} = \sum_{l=\max(0, j-n+1)}^{\min(j, n-1)} \sum_{m=\max(0, k-n+1)}^{\min(k, n-1)} \frac{\binom{n-1}{l} \binom{n-1}{j-l}}{\binom{2n-2}{j}} \frac{\binom{n-1}{m} \binom{n-1}{k-m}}{\binom{2n-2}{k}} \alpha_{lm} \sigma_{j-l} \sigma_{k-m}.$$

To construct the second term of $f(u, v)$, we write

$$\sigma(t) = \sum_{i=0}^{n-1} \sigma_i b_i^{n-1}(t), \quad (x'(t), y'(t)) = \sum_{i=0}^{n-1} n(\Delta x_i, \Delta y_i) b_i^{n-1}(t),$$

with $(\Delta x_i, \Delta y_i) = (x_{i+1} - x_i, y_{i+1} - y_i)$ for $i = 0, \dots, n - 1$, and thus obtain

$$\sigma(v)y'(u) - \sigma(u)y'(v) = \sum_{j=0}^{n-1} \sum_{k=0}^{n-1} n(\sigma_k \Delta y_j - \sigma_j \Delta y_k) b_j^{n-1}(u) b_k^{n-1}(v). \quad (13)$$

The method described in Section 2 then yields the coefficients γ_{jk} in the form

$$\frac{\sigma(v)y'(u) - \sigma(u)y'(v)}{u - v} = \sum_{j=0}^{n-2} \sum_{k=0}^{n-2} \gamma_{jk} b_j^{n-2}(u) b_k^{n-2}(v)$$

resulting from the division of (13) by $u - v$. To combine the first and second terms of $f(u, v)$ we must perform an n -fold degree elevation of the latter with respect to u and v , so both are expressed in the basis of degree $(2n-2, 2n-2)$. By the standard degree elevation algorithm [5], we obtain

$$\frac{\sigma(v)y'(u) - \sigma(u)y'(v)}{u - v} = \sum_{j=0}^{2n-2} \sum_{k=0}^{2n-2} \delta_{jk} b_j^{2n-2}(u) b_k^{2n-2}(v),$$

with coefficients defined for $0 \leq j, k \leq 2n - 2$ by

$$\delta_{jk} = \sum_{l=\max(0, j-n)}^{\min(j, n-2)} \sum_{m=\max(0, k-n)}^{\min(k, n-2)} \frac{\binom{n-2}{l} \binom{n}{j-l}}{\binom{2n-2}{j}} \frac{\binom{n-2}{m} \binom{n}{k-m}}{\binom{2n-2}{k}} \gamma_{lm}.$$

Finally, we can write $f(u, v)$ as

$$f(u, v) = \sum_{j=0}^{2n-2} \sum_{k=0}^{2n-2} (\beta_{jk} + d \delta_{jk}) b_j^{2n-2}(u) b_k^{2n-2}(v),$$

and the computation of $g(u, v)$ proceeds along analogous lines.

The solutions to the system $f(u, v) = g(u, v) = 0$, constructed as above, comprise not only the self-intersections of the untrimmed offset (10) but also its *cusps*, which arise [6] at the parameter values t satisfying

$$1 + \kappa(t) d = 0, \tag{14}$$

where

$$\kappa(t) = \frac{x'(t)y''(t) - x''(t)y'(t)}{\sigma^3(t)}$$

is the curvature of $\mathbf{r}(t)$. This can be seen as follows. Setting $u = t$, $v = t + \delta t$ we may expand equations (12) to first order in δt , obtaining

$$\begin{aligned} f(t, \delta t) &= \sigma^2 x' + d(\sigma y'' - \sigma' y') \\ &\quad + [\sigma(\frac{1}{2}\sigma x'' + \sigma' x') + \frac{1}{2}d(\sigma y''' - \sigma'' y')] \delta t + \dots = 0, \\ g(t, \delta t) &= \sigma^2 y' - d(\sigma x'' - \sigma' x') \\ &\quad + [\sigma(\frac{1}{2}\sigma y'' + \sigma' y') - \frac{1}{2}d(\sigma x''' - \sigma'' x')] \delta t + \dots = 0, \end{aligned}$$

where, for brevity, we omit the dependence of x, y, σ and their derivatives on t . Thus, the equations $f(t, \delta t) = g(t, \delta t) = 0$ are satisfied in the limit $\delta t \rightarrow 0$ (i.e., $u = v$) when t satisfies

$$\sigma^2 x' + d(\sigma y'' - \sigma' y') = \sigma^2 y' - d(\sigma x'' - \sigma' x') = 0.$$

Setting $\sigma^2 = x'^2 + y'^2$ and $\sigma' = (x'x'' + y'y'')/\sigma$, these conditions become

$$\sigma^3 x' + d x'(x'y'' - x''y') = \sigma^3 y' - d y'(x'y'' - x''y') = 0,$$

and since $(x', y') \neq (0, 0)$ for all t if $\mathbf{r}(t)$ is assumed to be regular, these reduce to the condition (14) for a cusp on the untrimmed offset.

Clearly, cusps of the untrimmed offset correspond to points lying on the symmetry axis $u = v$ of $f(u, v) = 0$ and $g(u, v) = 0$. They can be interpreted as limiting instances of the self-intersection condition (11), as $u \rightarrow v$. In general, cusps lie within parameter intervals $[u, v]$ delineated by proper self-intersections, with $v > u$, and it is not necessary to explicitly consider them in the offset trimming process. Algebraic methods based upon elimination theory [7] may, in principle, be employed to formulate univariate polynomials whose real roots identify only proper self-intersections of untrimmed offsets, but this approach incurs high-degree polynomials and is not well-suited to implementation in finite-precision arithmetic.

Example 5 Consider the offset at distance $d = -0.3$ to the quintic PH curve constructed as the “good” solution [4] to the Hermite interpolation specified by the initial and final control point pairs

$$\mathbf{p}_0 = (1.3, 1.0), \quad \mathbf{p}_1 = (1.9, 3.2) \quad \text{and} \quad \mathbf{p}_4 = (3.9, 0.6), \quad \mathbf{p}_5 = (2.5, 3.2).$$

This curve is illustrated, together with its offset, in Figure 10 below. In this case, the reduced difference polynomials (12) are of degree (8, 8) in (u, v) .

Figure 9 shows the quadtree localizations of $f(u, v) = 0$ and $g(u, v) = 0$, with resolution 2^{-8} . Using both to govern the subdivision, the subdomains over which $f(u, v)$ and $g(u, v)$ both exhibit coefficient sign changes are found to be: (1) the symmetric pair

$$\left[\frac{98}{256}, \frac{99}{256} \right] \times \left[\frac{227}{256}, \frac{228}{256} \right] \quad \text{and} \quad \left[\frac{227}{256}, \frac{228}{256} \right] \times \left[\frac{98}{256}, \frac{99}{256} \right],$$

not adjacent to the line $u = v$, that identify the proper self-intersection; (2) the symmetric pair

$$\left[\frac{198}{256}, \frac{199}{256} \right] \times \left[\frac{199}{256}, \frac{200}{256} \right] \quad \text{and} \quad \left[\frac{199}{256}, \frac{200}{256} \right] \times \left[\frac{198}{256}, \frac{199}{256} \right]$$

that are adjacent to the line $u = v$, identifying one of the two cusps; and the eight subdomains of the form

$$\left[\frac{141}{256}, \frac{142}{256} \right] \times \left[\frac{148}{256}, \frac{149}{256} \right], \dots, \left[\frac{148}{256}, \frac{149}{256} \right] \times \left[\frac{141}{256}, \frac{142}{256} \right]$$

that straddle the line $u = v$ symmetrically, identifying the other cusp. Taking the midpoint of the isolating subdomain for the self-intersection as a starting approximation, a few Newton–Raphson iterations yield rapid convergence to machine precision, identifying $(u, v) = (0.384450, 0.888147)$ as the parameter values satisfying (11). The self-intersection point is illustrated in Figure 12.

The behavior observed in Figure 5, with several isolating subdomains for the untrimmed offset cusps straddling the line $u = v$, is quite typical. Since $f(u, v) = 0$ and $g(u, v) = 0$ are symmetric about $u = v$, their tangents at points on this line must be orthogonal to it, and therefore the intersections of $f(u, v) = 0$ and $g(u, v) = 0$ on the line $u = v$ must be singular — i.e., with coincident tangents — rather than transversal. Consequently, it is preferable to identify the untrimmed offset cusps as the roots of the univariate equation (14), rather than as intersections of $f(u, v) = 0$ and $g(u, v) = 0$ with $u = v$.

Example 6 As a further example, consider the offset at distance $d = -0.45$ to the quintic PH curve constructed as the “good” solution corresponding to the initial and final control point pairs

$$\mathbf{p}_0 = (1.1, 3.2), \quad \mathbf{p}_1 = (2.0, 2.4) \quad \text{and} \quad \mathbf{p}_4 = (4.8, -0.8), \quad \mathbf{p}_5 = (1.6, 3.7).$$

This curve and its untrimmed offset are illustrated in Figure 12 below, and the reduced difference polynomials (12) are again of degree (8, 8).

Figure 11 shows the quadtree localizations of $f(u, v) = 0$ and $g(u, v) = 0$ for resolution 2^{-7} . Using both to guide the domain decomposition identifies the subdomains over which $f(u, v)$ and $g(u, v)$ both exhibit sign changes in their coefficients, as illustrated in Figure 12. These include two sets of subdomains straddling the line $u = v$, corresponding to cusps of the untrimmed offset, and the two subdomains

$$\left[\frac{32}{128}, \frac{33}{128} \right] \times \left[\frac{116}{128}, \frac{117}{128} \right] \quad \text{and} \quad \left[\frac{59}{128}, \frac{60}{128} \right] \times \left[\frac{101}{128}, \frac{102}{128} \right],$$

above $u = v$ (together with their symmetric counterparts below $u = v$), that identify proper self-intersections. Taking the subdomain midpoints as initial

values, a few Newton–Raphson iterations yield $(u, v) = (0.251707, 0.909006)$ and $(u, v) = (0.460449, 0.789455)$ as the parameter pairs satisfying (11). The self-intersections of the untrimmed offset are illustrated in Figure 12.

7 Closure

The Bernstein form of the bivariate reduced difference polynomials $f(u, v) = (x(u) - x(v))/(u - v)$ and $g(u, v) = (y(u) - y(v))/(u - v)$ associated with a polynomial curve $\mathbf{r}(t) = (x(t), y(t))$, $t \in [0, 1]$ can be employed to govern an efficient quadtree decomposition of the domain $(u, v) \in [0, 1]^2$, yielding a robust method for isolating the self-intersections of $\mathbf{r}(t)$ and computing the parameter value pairs u, v such that $\mathbf{r}(u) = \mathbf{r}(v)$. By generalizing the concept of a reduced difference polynomial to accommodate products of univariate polynomials, the methodology can be extended to compute self-intersections of rational curves, and of the offsets to Pythagorean–hodograph curves. The present study aims only to introduce the basic approach, and illustrate some key applications — as briefly discussed below, there are several improvements and extensions that may be worthy of further consideration.

Because of the inherent symmetry $f(u, v) = f(v, u)$ of reduced difference polynomials, and the fact that the *ordering* of the values in a pair (u, v) that identifies a self-intersection is immaterial, one need consider only solutions with either $u < v$ or $u > v$. Consequently, one may consider the formulation of reduced difference polynomials in the Bernstein basis specified in terms of barycentric coordinates over either of these triangular domains, rather than the tensor–product basis over $[0, 1] \times [0, 1]$. This formulation is somewhat more involved to implement, and will require a generalization of the quadtree decomposition scheme to the context of triangular domains, but may furnish some worthwhile benefits in terms of overall efficiency.

In computing self-intersections of the offsets to PH curves, it was noted that the solutions of the system $f(u, v) = g(u, v) = 0$ defined by the reduced difference polynomials also include the *cusps* of the untrimmed offset, which correspond to points on the symmetry line $u = v$. Since these cusps are not germane to the offset trimming process, their appearance as formal limiting solutions to the self-intersection problem is rather inconvenient. The division by $u - v$ in forming $f(u, v)$ and $g(u, v)$ does not eliminate them, and although they can be (numerically) computed as roots of the univariate equation (14), without further detailed investigations there is no obvious way to modify the

system $f(u, v) = g(u, v) = 0$ so as to eliminate them as solutions.

For optimum efficiency, it is desirable to terminate further subdivision of subdomains on which the conditions of the Kantorovich theorem (see the Appendix) for guaranteed convergence of the Newton–Raphson iterations to a unique solution hold. In this context, the primary challenge is to obtain tight bounds on the Lipschitz constant for the Jacobian matrix of the system of bivariate polynomial equations $f(u, v) = g(u, v) = 0$, as restricted to the subdomains $[u_1, u_2] \times [v_1, v_2]$ generated by the quadtree decomposition.

Finally, one may consider extensions of the methodology described herein to problems of higher dimensions — e.g., the self-intersections of polynomial parametric surfaces. This corresponds to tracing the one-dimensional set of solutions to a system $x(s, t) = x(u, v)$, $y(s, t) = y(u, v)$, $z(s, t) = z(u, v)$ of three equations in the four parametric unknowns (s, t, u, v) , and entails some formidable challenges. Specifically, a 4-dimensional analog of the quadtree decomposition scheme will be required, and the feasibility of a reduced system that eliminates the trivial solutions $(s, t) = (u, v)$ is not obvious.

Appendix: Kantorovich theorem

The Kantorovich theorem provides sufficient and necessary conditions for the convergence of Newton–Raphson iterations to a unique solution (u_*, v_*) of a system of non-linear equations

$$f(u, v) = g(u, v) = 0 \tag{15}$$

from a given starting approximation (u_0, v_0) within a prescribed domain \mathcal{D} . The following statement of the theorem is adapted from Ortega [15].

Let the independent variables and function values be specified by column vectors $\mathbf{w} = [u \ v]^T$ and $\mathbf{h}(u, v) = [f(u, v) \ g(u, v)]^T$, and let

$$\mathbf{J}(u, v) = \begin{bmatrix} f_u(u, v) & f_v(u, v) \\ g_u(u, v) & g_v(u, v) \end{bmatrix} \tag{16}$$

be the Jacobian matrix for the system (15), with inverse

$$\mathbf{J}^{-1}(u, v) = \frac{1}{\Delta(u, v)} \begin{bmatrix} g_v(u, v) & -f_v(u, v) \\ -g_u(u, v) & f_u(u, v) \end{bmatrix},$$

where $\Delta(u, v) = f_u(u, v)g_v(u, v) - f_v(u, v)g_u(u, v)$ is the determinant of $\mathbf{J}(u, v)$. Commencing with the starting approximation $\mathbf{w}_0 = [u_0 \ v_0]^T$ the Newton–Raphson iteration has the form

$$\mathbf{w}_{r+1} = \mathbf{w}_r - \mathbf{J}^{-1}(\mathbf{w}_r) \mathbf{h}(\mathbf{w}_r), \quad r = 0, 1, 2, \dots \quad (17)$$

Let $\|\mathbf{v}\|$ denote the norm of a vector \mathbf{v} , and $\|\mathbf{M}\|$ the corresponding norm of a matrix \mathbf{M} , namely

$$\|\mathbf{M}\| = \max_{\mathbf{v} \neq \mathbf{0}} \frac{\|\mathbf{M}\mathbf{v}\|}{\|\mathbf{v}\|}.$$

The theorem may be formulated in terms of these norms as follows.

Theorem 1 *For a starting approximation \mathbf{w}_0 in a domain \mathcal{D} , suppose that*

1. $\|\mathbf{J}^{-1}(\mathbf{w}_0)\| \leq \beta$,
2. $\|\mathbf{J}^{-1}(\mathbf{w}_0) \mathbf{h}(\mathbf{w}_0)\| \leq \eta$,
3. $\|\mathbf{J}(\mathbf{x}) - \mathbf{J}(\mathbf{y})\| \leq K \|\mathbf{x} - \mathbf{y}\|$ for all $\mathbf{x}, \mathbf{y} \in \mathcal{D}$,

for constants β, η, K and define

$$h = K\beta\eta, \quad \rho = \frac{1 - \sqrt{1 - 2h}}{h} \eta.$$

Then, if the conditions

$$h < \frac{1}{2} \quad \text{and} \quad \mathcal{S} = \{ \mathbf{w} \mid \|\mathbf{w} - \mathbf{w}_0\| \leq \rho \} \subset \mathcal{D}$$

hold, the iterations (17) remain inside the ball \mathcal{S} with center \mathbf{w}_0 and radius ρ , and converge quadratically to a unique solution $\mathbf{w}_* \in \mathcal{S} \cap \mathcal{D}$ of $\mathbf{h}(\mathbf{w}) = \mathbf{0}$.

The general p -norm of a vector $\mathbf{v} = (v_1, \dots, v_n)$ is defined by

$$\|\mathbf{v}\|_p = \left[\sum_{i=1}^n |v_i|^p \right]^{1/p},$$

and the simplest instances are the cases $p = 1$ and $p = \infty$, namely

$$\|\mathbf{v}\|_1 = \sum_{i=1}^n |v_i| \quad \text{and} \quad \|\mathbf{v}\|_\infty = \max_{1 \leq i \leq n} |v_i|.$$

For any other p , these norms impose the bounds

$$\frac{\|\mathbf{v}\|_1}{(n+1)^{1-1/p}} \leq \|\mathbf{v}\|_p \leq \|\mathbf{v}\|_1, \quad \|\mathbf{v}\|_\infty \leq \|\mathbf{v}\|_p \leq (n+1)^{1/p} \|\mathbf{v}\|_\infty.$$

The matrix norms corresponding to $p = 1$ and $p = \infty$ are likewise simple — if \mathbf{M} has elements M_{jk} for $1 \leq j, k \leq n$, they are given by

$$\|\mathbf{M}\|_1 = \max_{0 \leq k \leq n} \sum_{j=1}^n |M_{jk}| \quad \text{and} \quad \|\mathbf{M}\|_\infty = \max_{0 \leq j \leq n} \sum_{k=1}^n |M_{jk}|,$$

i.e., they are the greatest of the column sums and row sums of absolute values of the matrix elements, respectively. In the present context, the domain \mathcal{D} is $(u, v) \in [0, 1] \times [0, 1]$, and for brevity we focus on the $p = \infty$ norm.

For any starting approximation $\mathbf{w}_0 = [u_0 \ v_0]^T$ the quantities $\|\mathbf{J}^{-1}(\mathbf{w}_0)\|$ and $\|\mathbf{J}^{-1}(\mathbf{w}_0) \mathbf{h}(\mathbf{w}_0)\|$ can be directly computed, giving sharp values for the bounds β and η in the conditions 1 and 2 of the Kantorovich theorem. The non-linear dependence of the Jacobian (16) on u, v makes the determination of a sharp bound on the Lipschitz constant K in condition 3 more difficult, but an estimate can be obtained as follows. To first order, the change $\delta\mathbf{J}$ in the Jacobian corresponding to a change $\delta\mathbf{w} = [\delta u \ \delta v]^T$ in $\mathbf{w} = [u \ v]^T$ is

$$\delta\mathbf{J} = \begin{bmatrix} f_{uu} & f_{uv} \\ g_{uu} & g_{uv} \end{bmatrix} \delta u + \begin{bmatrix} f_{uv} & f_{vv} \\ g_{uv} & g_{vv} \end{bmatrix} \delta v.$$

Hence, noting that $0 \leq \delta u, \delta v \leq 1$ and invoking the triangle inequality, we find that $\|\delta\mathbf{J}\|_\infty$ is bounded (to first order in δu and δv) by the value

$$\max(|f_{uu}|\delta u + |f_{uv}|(\delta u + \delta v) + |f_{vv}|\delta v, |g_{uu}|\delta u + |g_{uv}|(\delta u + \delta v) + |g_{vv}|\delta v).$$

Moreover, since $\|\delta\mathbf{w}\|_\infty = \max(\delta u, \delta v)$ we may write

$$\|\delta\mathbf{J}\|_\infty \leq \max(|f_{uu}| + 2|f_{uv}| + |f_{vv}|, |g_{uu}| + 2|g_{uv}| + |g_{vv}|) \|\delta\mathbf{w}\|_\infty.$$

Thus, setting $\mathbf{x} = \mathbf{w}$ and $\mathbf{y} = \mathbf{w} + \delta\mathbf{w}$, and assuming that first-order terms are dominant, we obtain the estimate

$$K = \max(|f_{uu}| + 2|f_{uv}| + |f_{vv}|, |g_{uu}| + 2|g_{uv}| + |g_{vv}|)$$

for the Lipschitz constant in condition 3 of the Kantorovich theorem. Bounds on the absolute values of f_{uu}, f_{uv}, f_{vv} and g_{uu}, g_{uv}, g_{vv} for $(u, v) \in [0, 1] \times [0, 1]$ can be obtained from the absolute values of their Bernstein coefficients.

References

- [1] J. G. Alcazar, J. Caravantes, and G. M. Diaz–Toca (2015), A new method to compute the singularities of offsets to rational plane curves, *J. Comput. Appl. Math.* **290**, 385–402.
- [2] C–S. Chiang, C. M. Hoffmann, and R. E. Lynch (1991), How to compute offsets without self–intersections, SPIE Proceedings Vol. 1610: Curves and Surfaces in Computer Vision and Graphics II, 76–87.
- [3] G. Farin (1997), *Curves and Surfaces for Computer Aided Geometric Design*, 4th edition, Academic Press, San Diego.
- [4] R. T. Farouki (2008), *Pythagorean–Hodograph Curves: Algebra and Geometry Inseparable*, Springer, Berlin.
- [5] R. T. Farouki (2012), The Bernstein polynomial basis: a centennial retrospective, *Comput. Aided Geom. Design* **29**, 379–419.
- [6] R. T. Farouki and C. A. Neff (1990), Analytic properties of plane offset curves, *Comput. Aided Geom. Design* **7**, 83–99.
- [7] R. T. Farouki and C. A. Neff (1990), Algebraic properties of plane offset curves, *Comput. Aided Geom. Design* **7**, 101–127.
- [8] R. T. Farouki and C. A. Neff (1990), On the numerical condition of Bernstein–Bézier subdivision processes, *Math. Comp.* **55**, 637–647.
- [9] R. T. Farouki and T. Sakkalis (1990), Pythagorean hodographs, *IBM J. Res. Develop.* **34**, 736–752.
- [10] W. Feller (1950), *An Introduction to Probability Theory and its Applications*, Vol. 1, Wiley, New York.
- [11] M. Held (1991), *On the Computational Geometry of Pocket Machining*, Springer, Berlin.
- [12] M. Held (1998), Voronoi diagrams and offset curves of curvilinear polygons, *Comput. Aided Design* **30**, 287–300.

- [13] Y–J. Kim, J. Lee, M–S. Kim, and G. Elber (2012), Efficient offset trimming for planar rational curves using biarc trees, *Comput. Aided Geom. Design* **29**, 555–564.
- [14] I. Kucukoglu and Y. Simsek (2016), A note on generating functions for the unification of the Bernstein type basis functions, *Filomat* **30** (4), 985–992.
- [15] J. M. Ortega (1968), The Newton–Kantorovich theorem, *Amer. Math. Monthly* **75**, 658–660.
- [16] S. Osher and J. A. Sethian (1988), Fronts propagating with curvature–dependent speed: algorithms based on Hamilton–Jacobi formulations, *J. Comput. Phys.* **79**, 12–49.
- [17] H. Samet (1982), Neighbor finding techniques for images represented by quadtrees, *Comput. Graph. Image Proc.* **18**, 37–57.
- [18] H. Samet (1988), Hierarchical data structures and algorithms for computer graphics. I. Fundamentals, *IEEE Comput. Graph. Applic.* **8** (3), 48–68.
- [19] J–K. Seong, G. Elber, and M–S. Kim (2006), Trimming local and global self–intersections in offset curves/surfaces using distance maps, *Comput. Aided Design* **38**, 183–193.
- [20] J. A. Sethian (1999), *Level Set Methods and Fast Marching Methods: Evolving Interfaces in Computational Geometry, Fluid Mechanics, Computer Vision, and Materials Science*, Cambridge University Press.
- [21] Y. Simsek (2014), Generating functions for the Bernstein type polynomials: A new approach to deriving identities and applications for the polynomials, *Hacettepe J. Math. Stat.* **43** (1), 1–14.

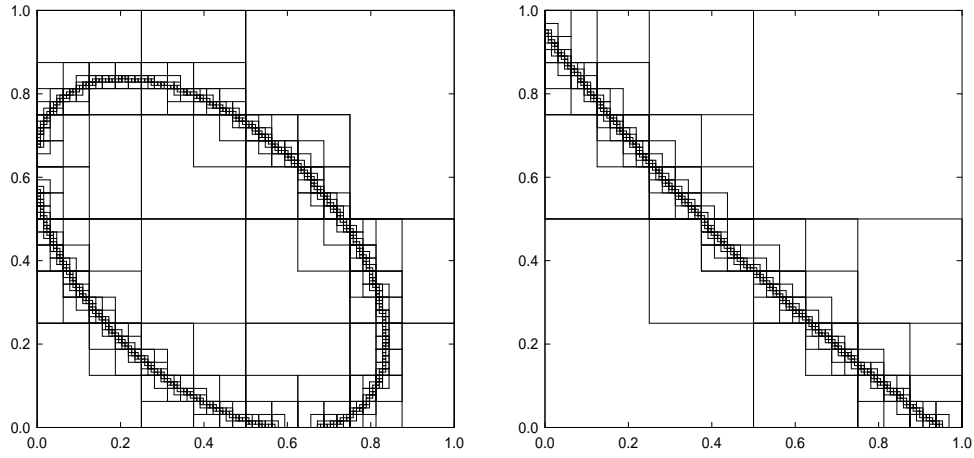


Figure 1: Quadtree localizations over the domain $(u, v) \in [0, 1] \times [0, 1]$ of the loci $f(u, v) = 0$ and $g(u, v) = 0$ defined by the reduced difference polynomials corresponding to $x(t)$ and $y(t)$, for the cubic test curve in Example 1.

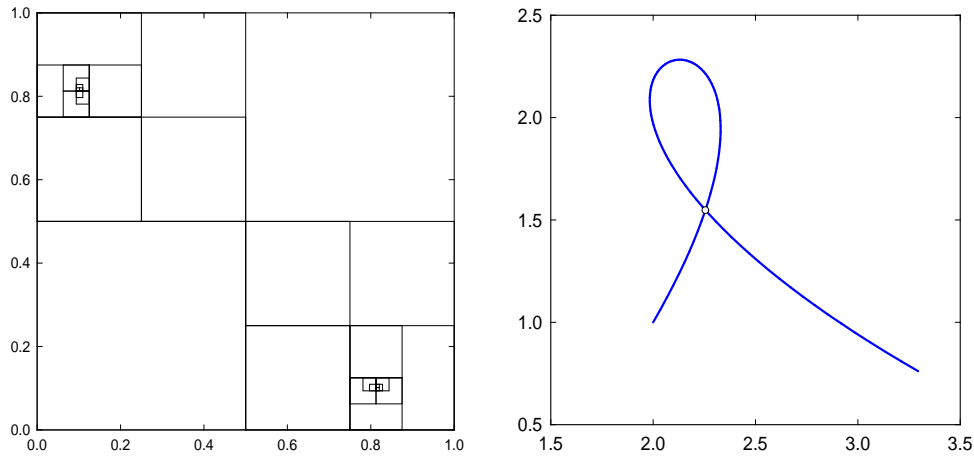


Figure 2: Left: rapid isolation of the self-intersection through simultaneous combination of the quadtree decompositions for $f(u, v) = 0$ and $g(u, v) = 0$. Right: the cubic curve in Example 1, showing the computed self-intersection.

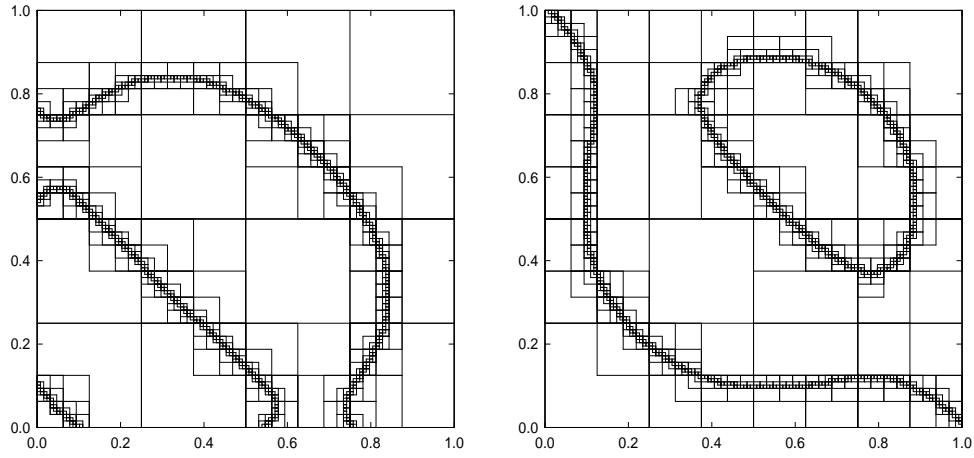


Figure 3: Quadtree localizations over the domain $(u, v) \in [0, 1] \times [0, 1]$ of the loci $f(u, v) = 0$ and $g(u, v) = 0$ defined by the reduced difference polynomials corresponding to $x(t)$ and $y(t)$, for the quintic test curve in Example 2.

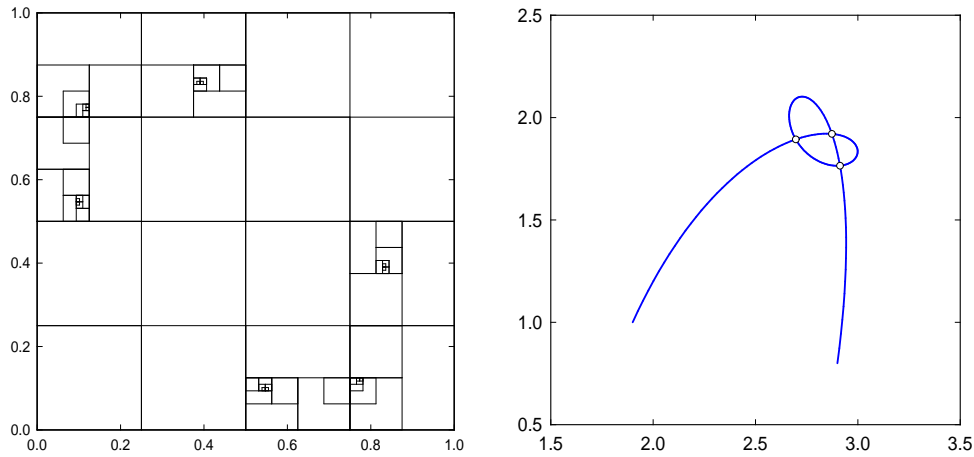


Figure 4: Left: rapid isolation of the self-intersections through simultaneous combination of the quadtree decompositions for $f(u, v) = 0$ and $g(u, v) = 0$. Right: the quintic curve in Example 2, showing the three self-intersections.

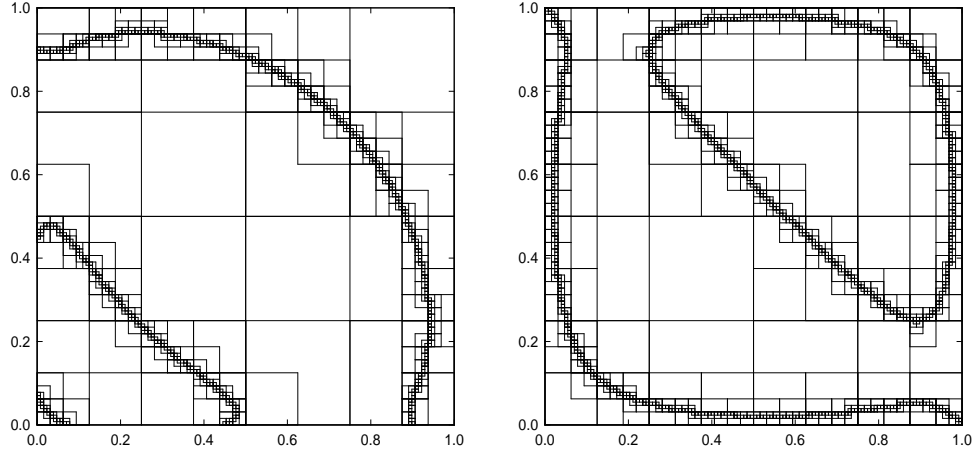


Figure 5: Quadtree localizations over the domain $(u, v) \in [0, 1] \times [0, 1]$ of the loci $f(u, v) = 0$ and $g(u, v) = 0$ defined by the reduced difference polynomials corresponding to $x(t)$ and $y(t)$, for the rational test curve in Example 3.

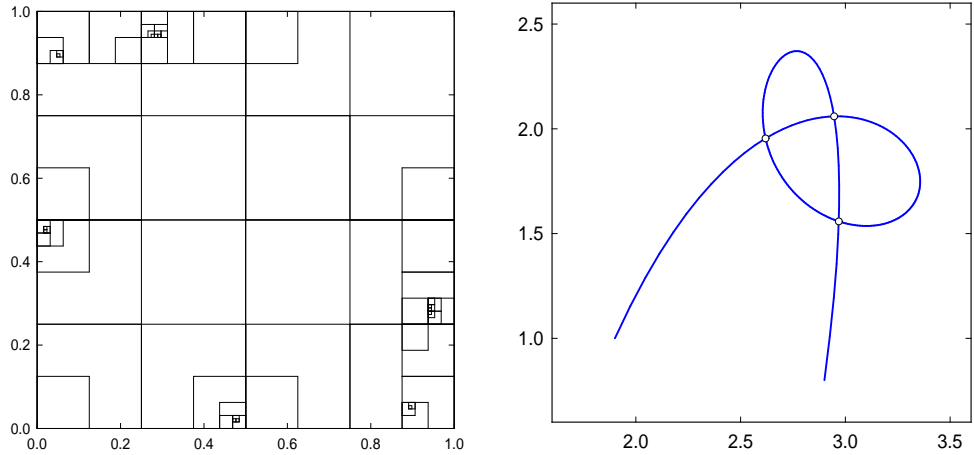


Figure 6: Left: rapid isolation of the self-intersections through simultaneous combination of the quadtree decompositions for $f(u, v) = 0$ and $g(u, v) = 0$. Right: the rational curve in Example 3, showing the three self-intersections.

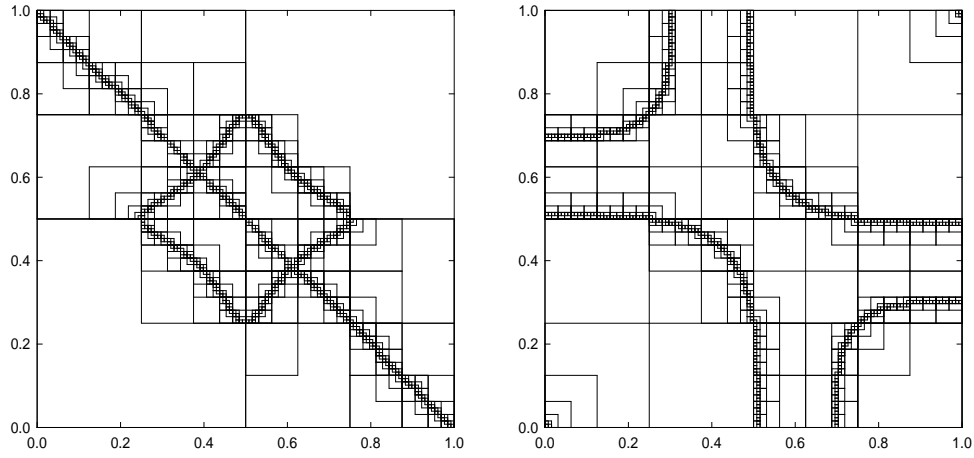


Figure 7: Quadtree localizations over the domain $(u, v) \in [0, 1] \times [0, 1]$ of the loci $f(u, v) = 0$ and $g(u, v) = 0$ defined by the reduced difference polynomials for the rational quartic test curve with a triple point in Example 4.

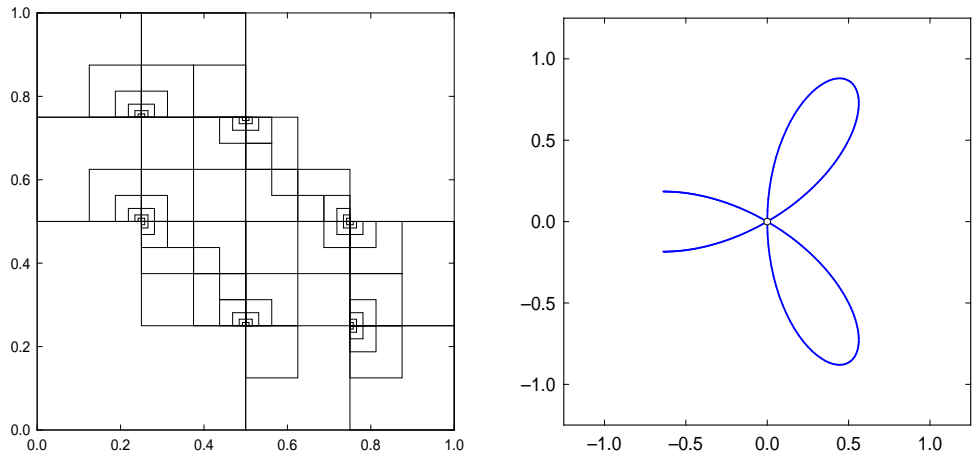


Figure 8: Left: isolating the parameter pairs $(\frac{1}{4}, \frac{1}{2})$, $(\frac{1}{2}, \frac{3}{4})$, $(\frac{1}{4}, \frac{3}{4})$ that identify the triple point by combining the quadtree decompositions of $f(u, v) = 0$ and $g(u, v) = 0$. Right: the rational quartic curve, illustrating the triple point.

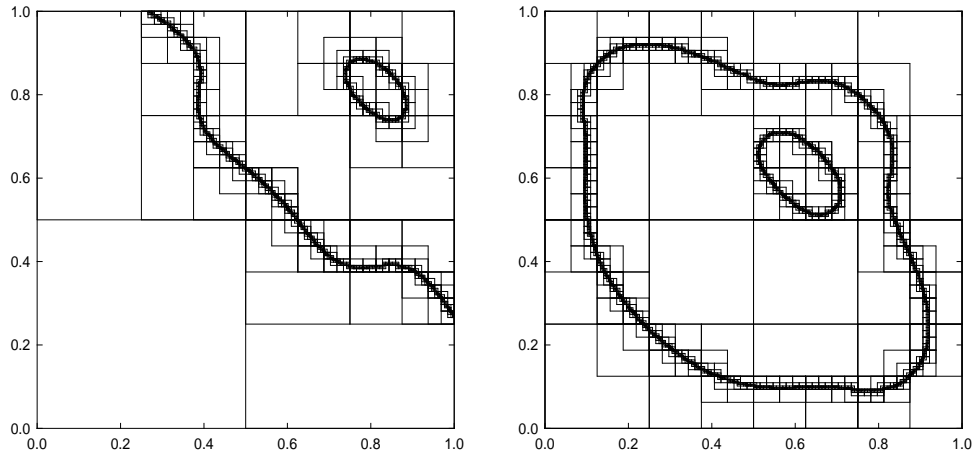


Figure 9: Quadtree localizations over the domain $(u, v) \in [0, 1] \times [0, 1]$ of the loci $f(u, v) = 0$ and $g(u, v) = 0$ defined by the reduced difference polynomials corresponding to $x(t)$ and $y(t)$, for the untrimmed offset at distance $d = -0.3$ to the quintic Pythagorean-hodograph test curve in Example 5.

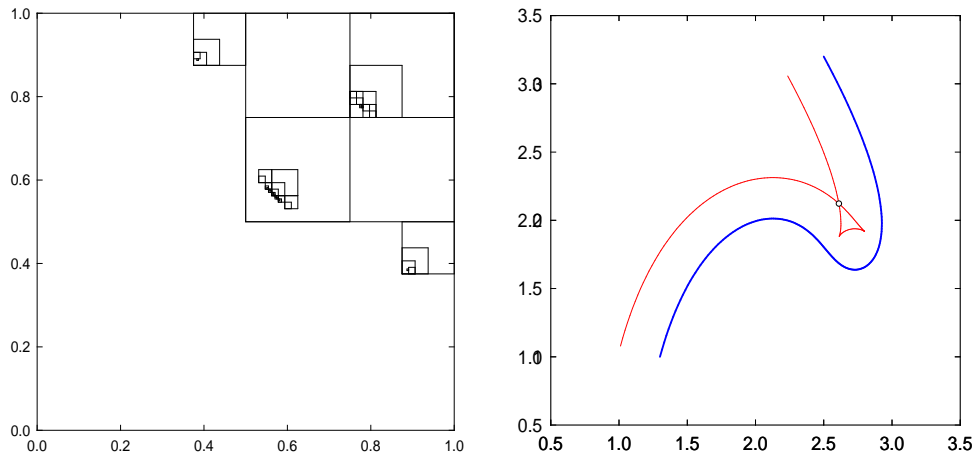


Figure 10: Left: rapid isolation of the self-intersection through the combined quadtree decomposition of $f(u, v) = 0$ and $g(u, v) = 0$. Isolating subdomains that straddle the line $u = v$ identify cusps, while those removed from this line identify proper self-intersections. Right: the quintic PH curve in Example 5, illustrating the two cusps and self-intersection of the untrimmed offset.

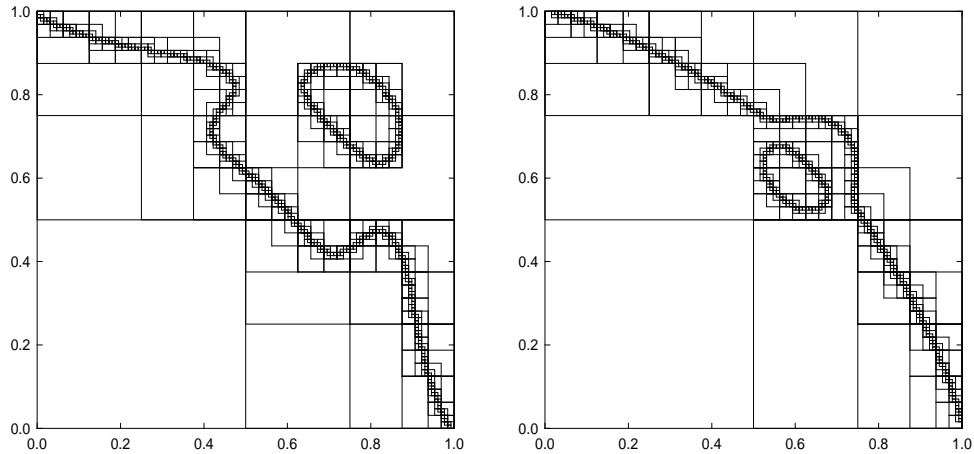


Figure 11: Quadtree localizations over the domain $(u, v) \in [0, 1] \times [0, 1]$ of the loci $f(u, v) = 0$ and $g(u, v) = 0$ defined by the reduced difference polynomials corresponding to $x(t)$ and $y(t)$ for the untrimmed offset at distance $d = -0.45$ to the quintic Pythagorean-hodograph test curve in Example 6.

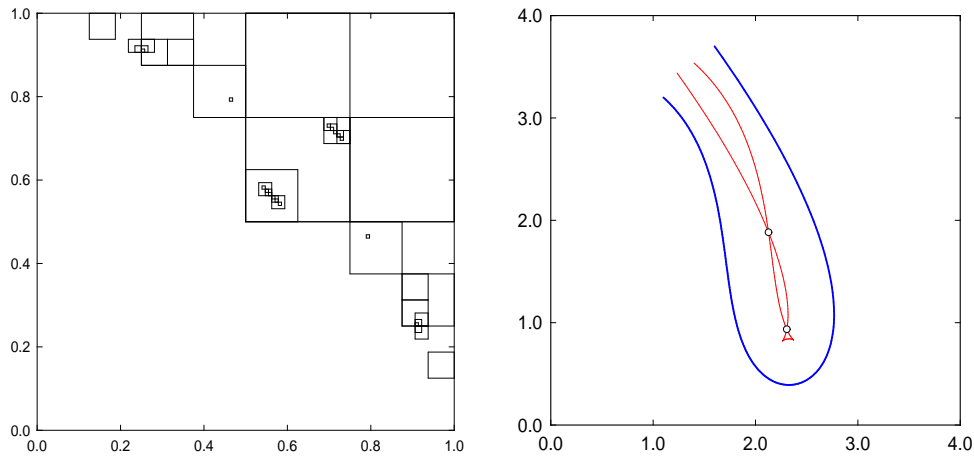


Figure 12: Left: rapid isolation of the self-intersections through the combined quadtree decomposition of $f(u, v) = 0$ and $g(u, v) = 0$. Isolating subdomains that straddle the line $u = v$ identify cusps, while those removed from this line identify proper self-intersections. Right: the quintic PH curve in Example 6, illustrating the two cusps and self-intersections of the untrimmed offset.